INFLUENCE OF GEOMETRY PARAMETERIZATION IN AERODYNAMIC SHAPE DESIGN OF AERONAUTICAL CONFIGURATIONS BY EVOLUTIONARY ALGORITHMS

Daniel González Juárez, Esther Andrés Pérez**, Mario Jaime Martin Burgos*, Leopoldo Carro-Calvo*** and Sancho Salcedo Sanz****

** Fluid Dynamics Branch, Spanish National Institute for Aerospace Technology (INTA)*
Ctra. Ajalvir, km. 4., 28850 Torrejón de Ardoz, Spain
*** Fluid Dynamics Branch, Spanish National Institute for Aerospace Technology (INTA/ISDEFE) &*
Technical University of Madrid (UPM)
Ctra. Ajalvir, km. 4., 28850 Torrejón de Ardoz, Spain
**** Department of Signal Theory and Communications, University of Alcalá (UAH)*
Ctra. Madrid-Barcelona km. 33.6, Alcalá de Henares (Spain)

Abstract

The development of an automatic geometry optimization tool for efficient aerodynamic shape design, supported by Computational Fluid Dynamic (CFD) methods is nowadays an active research field, as can be observed from the increasing number of scientific publications during the last years. In particular, the choice of a proper parameterization is critical for the performing of the optimizations. This paper focuses on the application of an optimization framework based on the combined use of the surrogate modelling techniques, evolutionary algorithms and volumetric Non Uniform Rational B-splines (NURBS). More specifically, this work aims to analyze how sensitive this approach is to the number of the control points. Some conclusions will be drawn on the influence of the number of design variables in order to provide optimal shapes in an efficient manner. To do this, two well-known aeronautical test cases have been analyzed: the two-dimensional RAE2822 airfoil and the three-dimensional DPW-W1 wing in transonic flow conditions.

1. Introduction

Industrial application of automatic aerodynamic shape optimization tools has still to face several challenges, as for instance, how to tackle integrated components, how to allow deformations in certain regions (as intersections between wing and fuselage or pylon/nacelle) or how to reduce the computational cost usually required for performing aerodynamic design optimization. In addition, the selection of the design parameters is a crucial step, which has to be chosen at the beginning of the process, and strongly determines the range of solutions and performance of the optimization algorithm. Therefore, the selection of an adequate parameterization will greatly affect both the efficiency of the optimization process and the optimal solutions.

A high number of design variables, which in the approach proposed in this work are the NURBS control points, tend to create rough surfaces and undesired loose of smoothness. Also the surrogate prediction is highly influenced by the number of inputs. The study of the correlation among these issues is essential in order to accomplish successful optimizations suitable for its implementation in the aeronautical industry.

The aim of this work is to provide a comprehensive study about how the selected parameterization and number of design variables affect the convergence, surrogate prediction accuracy and results of such surrogate-based global optimization methods (SBGO). This study aims to drive some conclusions and to propose certain rules for a suitable geometry parameterization and discretization settings, leading to better optimizations procedures.

This work is under the scope of the GARTEUR Action Group (AD/AG52), with the objective of providing a comprehensive survey about different surrogate methods for surrogate-based aerodynamic shape optimization, started at the beginning of 2013. Within this Group, research activities are planned over a three-year period, with the objective of performing a fair comparison between different surrogate modeling methods applied to the aerodynamic optimization of baseline geometries, sharing the parameterization (volumetric NURBS) and mesh deformation algorithms. The work presented complements the research activities performed in the mentioned European group.

2. Previous work

In the field of aircraft design, parameterization techniques have a significant impact on the stability, efficiency and performance of the optimization. There have been several attempts to compare different parameterization methods [1], [2] based on key characteristics, such us flexibility, complexity, practical implementability, uniform parameter sensitivity, orthogonality (defined as one shape is identified by a unique set of parameters), among other characteristics. Parameterization methods can be roughly classified as descriptive and differential. Descriptive methods provides a set of design variables that describes the geometry. For example, the parametric section (PARSEC) [3], proposed by Sobiecky, describes an airfoil with eleven geometric key parameters. More recently, the class/shape function transformation (CST) [4], proposed by Kulfan, describes aircraft components surfaces as a product of a class function and a shape function created from key geometric parameters, such as leading edge radius, trailing edge, and closure to a specified aft thickness. Non-Uniform Rational B-Splines (NURBS) [5] [6] is a generic representation widely employed by modern computer aided design programs (CAD). This approach does not provide an intuitive physical meaning, as the previous ones, but it allows to explore the design space for unconventional and off-the-book designs. On the other hand, differential methods employ a baseline geometry and then apply deformations based on a shape function. These methods are in general easier to implement into the computational grid. For example, a profile can be accurately represented by a NURBS curve with 12 to 18 control points, but finding such curve can be a process that requires great expertise, and for complex geometries could be impractical. One of the earliest design variables in this category are the Hicks-Henne bump functions. Another simple technique is Free Form Deformation (FFD) [7], which envelops the geometry inside a lattice box or hull and performs global deformations of the space inside. The method is analog to NURBS surface in a sense that deformations are controlled by the movement of control points. The most common form of FFD employs Bernstein polynomials, which allow to directly link the spatial coordinates to the parametric coordinates through linear transformation, provided some rules how the box is build are followed. More recently, the Control Box [8] approach employs volumetric NURBS as basis functions. This technique requires the additional effort to calculate the parametric coordinates from the spatial coordinates through an appropriated inversion point algorithm, but confers important advantages over FFD, such as deformation locality, arbitrary set up of the control points, selection of the smoothness, and order of the interpolation, while achieving the same deformation characteristics as conventional surface NURBS.

3. Proposed approach

3.1. Geometry parameterization of airfoil and wing

Non-Rational Uniform B-Splines (NURBS) have demonstrated to be able to accurately represent a large family of geometries. In aerodynamic design, provides smooth surfaces while maintaining some deformation locality [9]. In addition, the optimized surface at the end of the optimization process has the correct format to feed directly the CAD and grid generation applications. However, the use of surface NURBS can be impractical, because very frequently requires the additional effort to develop a surface representation that fits the original geometry, with an appropriated arrange of control points for the optimization. An alternative approach is to envelop the geometry in a volumetric NURBS, which maintain the deformation properties of a conventional 2-dimensional surface, but with the advantage that control points can be set up arbitrarily.

From a mathematical point of view, NURBS surfaces are defined as the tensor product of three NURBS curves, defining a volumetric region, where the deformation is governed by the movement of control points:

$$S(\xi,\eta,\mu) = \frac{\sum_i^I \sum_j^J \sum_k^K U_{i,n}(\xi)\, V_{i,n}(\eta)\, W(\mu)\, C_{ijk}}{\sum_i^I \sum_j^J \sum_k^K U_{i,n}(\xi)\, V_{i,n}(\eta)\, W(\mu)} \tag{1}$$

where C are the control points , $\xi, \eta, and\ \mu$ are the parametric coordinates, and $U, V, and\ W$ are the basis functions which are calculated using the following expression:

$$U_{i,1}(\xi) = \begin{cases} 1\ if\ u_i \leq \xi < \ u_{i+1} \\ 0 \quad otherwise \end{cases} \tag{2}$$

$$U_{i,k}(\xi) = \frac{(\xi - u_i)U_{i,k-1}(\xi)}{u_{i+k-1} - u_i} + \frac{(u_{i+k} - \xi)U_{i+1,k-1}(\xi)}{u_{i+k} - u_{i+1}}$$

The basis coefficients are calculated from the knot vectors $\overline{U}$, $\overline{V}$ and $\overline{W}$, which are a sequence of real numbers. Basis functions are equal to zero everywhere except for an interval delimited by the order of the NURBS, defining the area of influence of each control point [10]. The most common implementation of the control box is to employ uniform basis, which can be obtained with a knot sequence as:

$$\{\underbrace{0,\dots,0}_{p+1},\frac{1}{N},\dots,\frac{i}{N},\dots,\frac{N-1}{N},\underbrace{1,\dots,1}_{p+1}\} \tag{3}$$

First order is equivalent to a linear interpolation, while second and third orders provide derivative and curvature continuity. In this work, the geometries are parameterized with a volumetric b-spline, also called control box (for both RAE 2822 and DPW wing), with third order, and the design variables will be the vertical displacements (z axis) of the control points. Figure 1 and Figure 2 shows the selected parameterization.

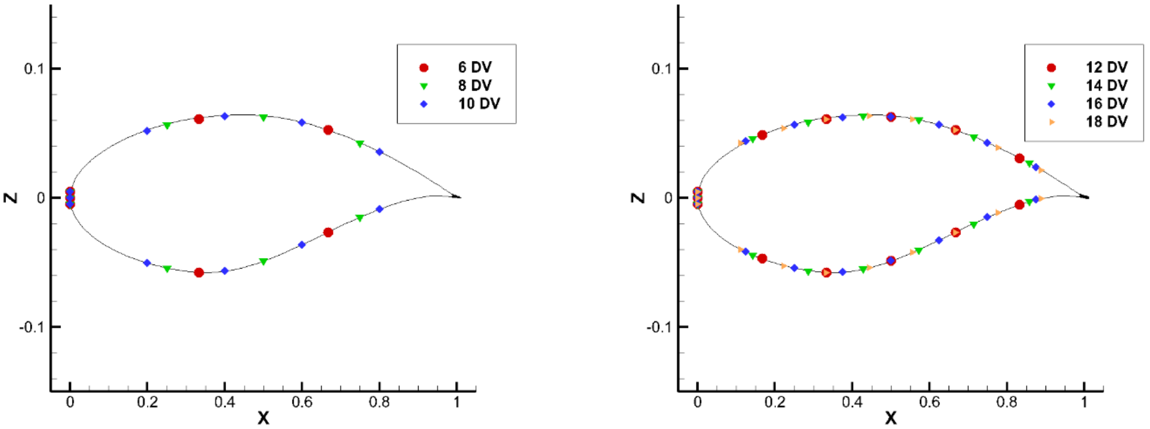

Figure 1. Geometry parameterization of the RAE 2822 airfoil by volumetric NURBS

To clarify, there are additional control points at the trailing edge that are kept fixed, in order to maintain the angle of attack; so the are not considered design variables. The design variables on the three-dimensional wing are those control points on the surface.

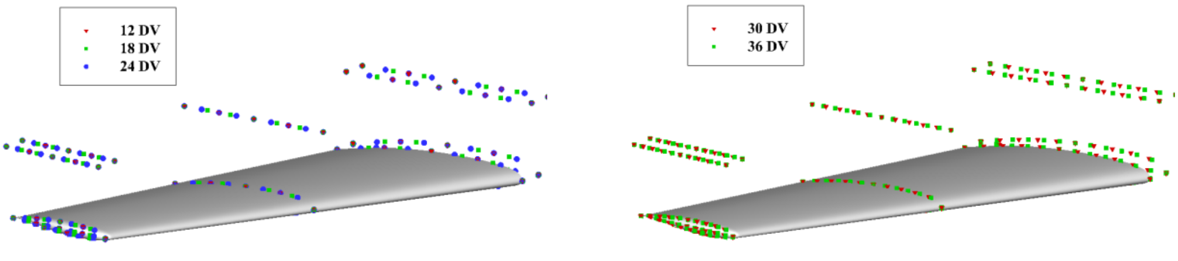

Figure 2. Geometry parameterization of the DPW wing by volumetric NURBS

3.2. Evolutionary Algorithm

Evolutionary Algorithms (EAs) are bio-inspired methods that mimic the behavior of natural evolution to solve complex optimization problems. The main elements of an EA are the solution coding, the selection operator and the crossover and mutation operators. The EA implemented for this work has the following characteristics:
1. Solution coding: The solutions are coded as a vector of real values from 0 to 1. Each element of the vector represents the value of a normalized parameter.
2. Selection operator: In the proposed EA, the selection operator is applied by replacing a portion of the current generation by new individuals generated from parents [11]. It is considered the replacement of the individuals in the population with fitness value under the population's mean fitness. First, the mean population fitness is calculated as:

$$\bar{g} = \frac{1}{\xi}\sum_{k=1}^{\xi} g_k \tag{4}$$

where g_k is the fitness of the k^{th} individual and ξ represents the number of individuals in the population. Every individual in the population with a value of fitness under $\bar{g}$ is discarded, and substituted by a new individual obtained with the crossover operator.
3. Crossover operator: generates a new individual from the values of two parents selected randomly from the survival individuals. A multipoint crossover which selects the value of one of the parents with probability 0.5 is applied.
4. Mutation operator: The values of each new individual are mutated with probability $1/Np$, where Np is the number of parameters to be optimized. This operator changes the initial individual by using this formula:

$$V_i = V_i \cdot (1 + U \cdot \alpha) \tag{5}$$

where V_i represents each one of the parameters to optimize, U is an uniform noise [0-1] and α is a value which represent the mutation level. Three values of α have been used, 1, 0.1 and 0.01, randomly selected for each new individual with probability ${}^{1}/_{3}$. It can be observed that α=1 represents a strong change on the initial value. On the other hand, $\alpha = 0.01$ implies a change of 1% of the initial value, allowing a local search over this parameter.

3.3. Objective function approximation using Support Vector Machines

Support Vector Machines for regression (SVMr) are a powerful tool used on the machine learning field, and as a modelling tool for a large amount of regression problems on engineering. The SVMr can be solved as a convex optimization problem using kernel theory to face nonlinear problems. The SVMr consider not only the prediction error but also the generalization of the model.
The SVMr consist of training a model with the form $y = w^T\,\Phi(x) + b$ given a set of parameters $C = \{(x_i, y_i\ ), i = 1,2, \ldots, l\}$, to minimize a general risk function of the form:

$$R[f] = \frac{1}{2}\|w\|^2 + \frac{1}{2}C\sum_{i=1}^{l} L(y_i, f(x)) \tag{6}$$

where w controls the smoothness of the model, $\Phi(x)$ is a function of projection of the input space to the feature space, b is a parameter of bias, x_i is a feature vector of the input space with dimension N, y_i is the output value to be estimated and $L(y_i, f(x))$ is the loss function selected. In this paper, the L1-SVR (L1 support vector regression) is used, characterized by an ε-insensitive loss function

$$L\big(y_i, f(x)\big) = |y_i - f(x_i)|_\varepsilon \tag{7}$$

In order to train this model, it is necessary to solve the following optimization problem

$$\min\left(\frac{1}{2}\|w\|^2 + \frac{1}{2}C\sum_{i=1}^{l} \xi_i + \xi_i^*\right) \tag{8}$$

subject to:

$$\begin{aligned} y_i - w^T\Phi(x) - b \leq \varepsilon + \xi_i, i = 1, \dots, l \\ -y_i + w^T\Phi(x) + b \leq \varepsilon + \xi_i^*, i = 1, \dots, l \\ \xi_i, \xi_i^* \geq 0, i = 1, \dots, l \end{aligned} \tag{9}$$

To do this, a dual form is usually applied, obtained from the minimization of the Lagrange function that joins the function to minimize and the restrictions. The dual form is:

$$\max(-\frac{1}{2}\sum_{i,j=1}^{l}(\alpha_i + \alpha_i^*)(\alpha_j + \alpha_j^*)K(x_i + x_j) - \varepsilon\sum_{i=1}^{l}(\alpha_i + \alpha_i^*) + \sum_{i=1}^{l} y_i(\alpha_i + \alpha_i^*) \tag{10}$$

subject to:

$$\sum_{i=1}^{l}(\alpha_i - \alpha_i^*) = 0;\ \alpha_i, \alpha_i^* \in [0, C] \tag{11}$$

In addition to the restrictions, also must be taken in account the Karush-Kuhn-Tucker conditions and obtain the bias value. In the dual formulation we must emphasize the apparition of the kernel function $K(x_i, x_j)$, which is equivalent to the scalar product $\langle \Phi(x_i\ ), \Phi(x_j\ )\rangle$. In our case, the kernel function is a Gaussian function:

$$K(x_i, x_j) = \exp(-\gamma \cdot \|x_i - x_j\|^2) \tag{12}$$

The final form of the regression model depends on the Lagrange multipliers α_i, α_i^*, following the expression:

$$f(x)\sum_{i=1}^{l}(\alpha_i - \alpha_i^*)K(x_i, x) + b \tag{13}$$

In this way, the SVMr model depends on three parameters,ε, C and γ. The ε parameter controls the error margin permitted for the model, as can be seen in equations (8), (9), the C parameter controls the number of outliers allowed on the optimization of the function equation (8). Finally the γ parameter determines the Gaussian variance for the kernel. Depending on the selection of these values, the model can have a different performance. To obtain the best SVM performance, a search of the most suitable combination of these three parameters must be carried on, usually by using cross validation techniques over the training set. To reduce the computational time of this process, different methods have been proposed in the literature to reduce the search space related to these parameters. In this case, it has been applied the one developed by Ortiz-García et al [12] which has proven to require pretty short search times.

3.4. Flowchart of the proposed approach

In this work, a surrogate-based global optimization method with adaptive sampling is applied, called “The intelligent Estimation Search with Sequential Learning (IES-SL)”. This method allows performing an efficient adaptive sampling guiding the optimization algorithm towards the most promising regions of the design space. The flowchart of the proposed approach is displayed in Figure 3.

The key feature of this approach is to use the surrogate model to estimate the location of the optimum in the real function. To do this, an evolutionary optimization search is applied over the surrogate, obtaining an estimated value of the real minimum position (an “intelligent guess”) [13]. Each of the estimations of the optimum location gives us a new sampling point (it means a new geometry that is also analyzed using the high fidelity CFD solver). Within a try-and-error cycle, the surrogate proposes a new design which is again evaluated by the CFD solver and then, in a sequential learning, the surrogate model is enriched with the associated cost function.

When the maximum number of iterations is reached, the optimum design is obtained as the best parameters on the database. In this way, we ensure that the design obtained is optimum with respect to the simulator system (CFD solver) and not only to the surrogate model.

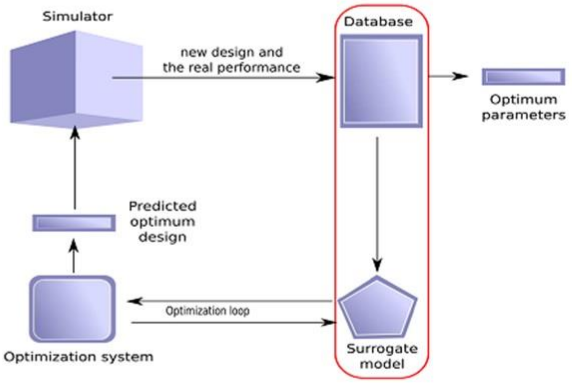

Figure 3. Flowchart of the SBO process

4. Numerical results

4.1. Test cases definitions

The fluid flow over the geometries of interest is simulated with the TAU Code [14] from the German Aerospace Center (DLR). The unsteady TAU Code solves the compressible, three-dimensional Reynolds-Averaged Navier-Stokes equations using a finite volume formulation. The TAU-Code is based on a hybrid unstructured-grid approach, which makes use of the advantages of semi-structured prismatic grids in the viscous shear layers near walls, while providing the flexibility offered by creating tetrahedral elements in the surrounding flow volume. A dual-grid approach with an edge based data structure is used in order to make the flow solver independent from the cell types used in the initial grid.

The proposed IES-SL approach is applied to the aerodynamic shape optimization of a RAE2822 airfoil and a DPW-W1 wing, with the problem formulation defined on Table 1.

Table 1. Test cases definition

	#Design variables	Flow conditions DP1	Flow conditions DP2	Objective function(OF)	Aerodynamics constraints and penalties	Geometric constraints
RAE 2822 airfoil	6,8,10, 12,14,16, 18	M=0.734 Re=6.5 x 10^6 AoA=2.8° SA	M=0.754 Re=6.2 x 10^6 AoA=2.12° SST	$Min\ (C_D/C_L)$	Prescribed minimum lift coefficient $C_l^0\|_k: C_l\|_k \geq C_l^0\|_k$ Prescribed minimum pitching coefficient $C_m^0\|_k: C_m\|_k \geq C_m^0\|_k$ Drag penalty: if constraint on minimum pitching moment is not satisfied, the penalty will be 1 drag count per 0.01 in ΔC_m	Limit: +/- 20% of the initial control points values
DPW-W1 wing	12,18,24, 30, 36	M=0.8 AoA=0^0 Euler	-			

A total budget of 100 CFD computations for RAE 2822 airfoil and 300 CFD computations for DPW-W1 wing was defined.

4.2. Metamodel obtention (SVMr)

The surrogate model based on SVMr is built following the approach displayed in Figure 3. The validation strategy is explained in [15]. The obtained mean square errors (MSE) when predicting the objective function are displayed in Table 2. The proposed sampling method is compared to a Latin Hypercube Sampling (LHS) method. It can be seen that there are not significant differences in accuracy.

Table 2. Validation of the surrogate model based on SVMr.

Sampling method	Problem	Objective	C_L constraint	C_M constraint	MSE
EA-SVM	RAE 2822	min (C_D/ C_L)	No	No	0.0766
EA-SVM	RAE 2822	min (C_D/ C_L)	No	Yes	0.0599
EA-SVM	RAE 2822	min (C_D/ C_L)	Yes	Yes	0.2089
EA-SVM	DPW-W1	min (C_D/ C_L)	Yes	Yes	0.0072
LHS	DPW-W1	min (C_D/ C_L)	Yes	Yes	0.0078
EA-SVM	DPW-W1	min (C_D/ C_L)	Yes	No	0.0075
LHS	DPW-W1	min (C_D/ C_L)	Yes	No	0.0075

4.3. Optimization of a RAE2822 airfoil

In this section, the approach is applied to the optimization of a RAE2822 airfoil, as defined in 4.1. Table 3 and Figure 4 show the objective function (OF) and the aerodynamic efficiency (AE) of the original and optimized geometries.

Table 3. RAE 2822 optimization results

	C_D		C_L		C_M		OF	AE	
	$DP1$	$DP2$	$DP1$	$DP2$	$DP1$	$DP2$		$DP1$	$DP2$
original	0.0188	0.0204	0.8008	0.6606	-0.0953	-0.1022	1	42.51	32.36
6 dv	0.0143	0.0149	0.8078	0.7589	-0.0902	-0.0967	0.7481	56.64	44.11
8 dv	0.0134	0.0120	0.8464	0.7067	-0.0941	-0.0992	0.6113	63.18	58.88
10 dv	0.0135	0.0119	0.8451	0.7245	-0.0885	-0.0959	0.6048	63.04	60.47
12 dv	0.0132	0.0117	0.8306	0.7065	-0.0863	-0.0942	0.6077	62.75	60.15
14 dv	0.0127	0.0118	0.8223	0.6940	-0.0941	-0.1008	0.6051	64.39	58.84
16 dv	0.0131	0.0126	0.8394	0.6820	-0.0953	-0.0989	0.6323	63.81	54.10
18 dv	0.0138	0.0129	0.8517	0.6898	-0.1018	-0.1038	0.66511	61.49	53.32

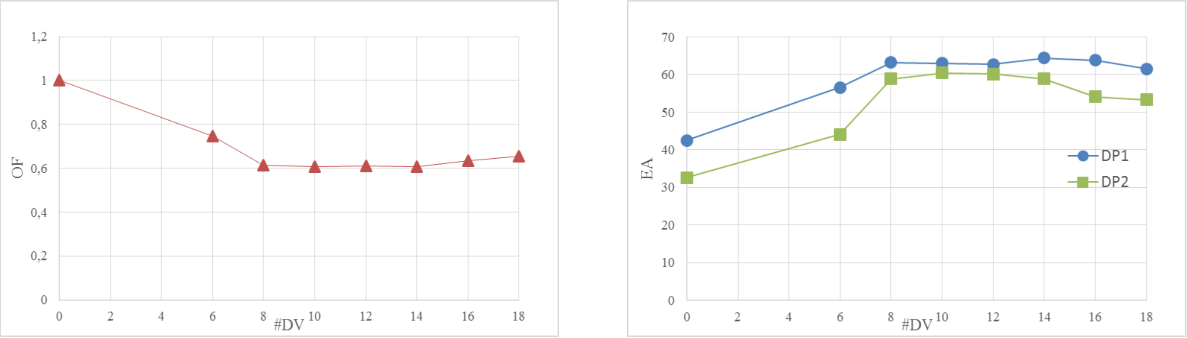

Figure 4. Evolution of OF and AE with #DV for RAE 2822 optimization

For this test case, a multipoint optimization has been executed for each parameterization. Results show an optimum within 10DV, reaching an improvement by ~40%, while fulfilling the constraints imposed to C_L and C_M.

Figure 5 shows the shapes and pressure coefficient distributions of the original and optimized geometries.

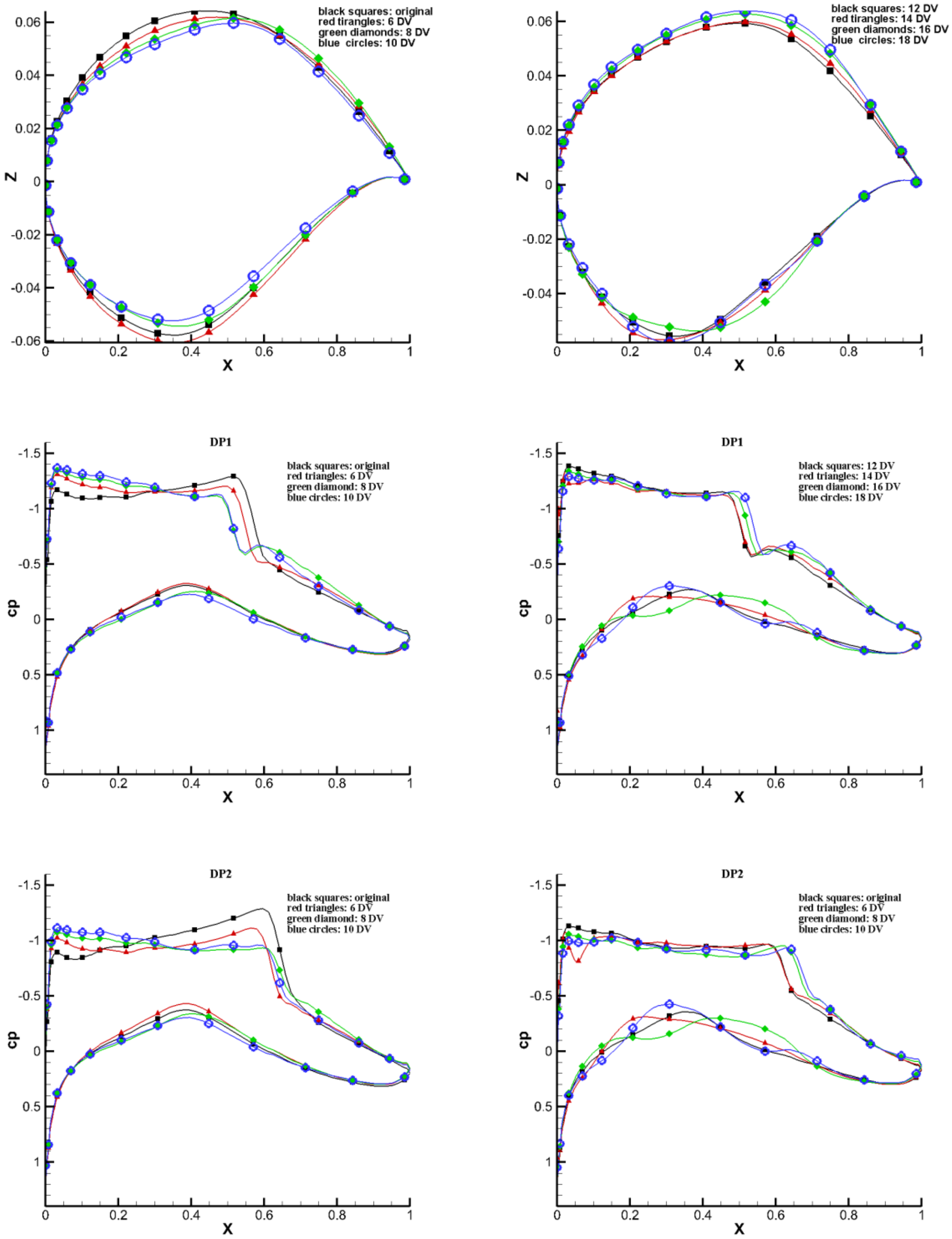

Figure 5. RAE 2822 optimization results

4.4. Optimization of a DPW-W1 wing

In this section the approach is applied to the optimization phase of a DPW-W1 wing, as defined in section 4.1. Table 4 and Figure 6 show the objective function (OF) and the aerodynamic efficiency (AE) function and optimized geometries.

Table 4. DPW-W1 wing optimization results

	C_D	C_L	C_{My}	***OF***	***AE***
original	0.0307	0.5984	-0.0286	1	19.48
12 dv	0.0229	0.5987	-0.0266	0.7373	26.14
18 dv	0.0217	0.5990	-0.0260	0.7069	27.58
24 dv	0.0213	0.5981	-0.0261	0.6964	28.06
30 dv	0.0214	0.5986	-0.0260	0.6962	27.99
36 dv	0.0228	0.5971	-0.0250	0.7361	26.81

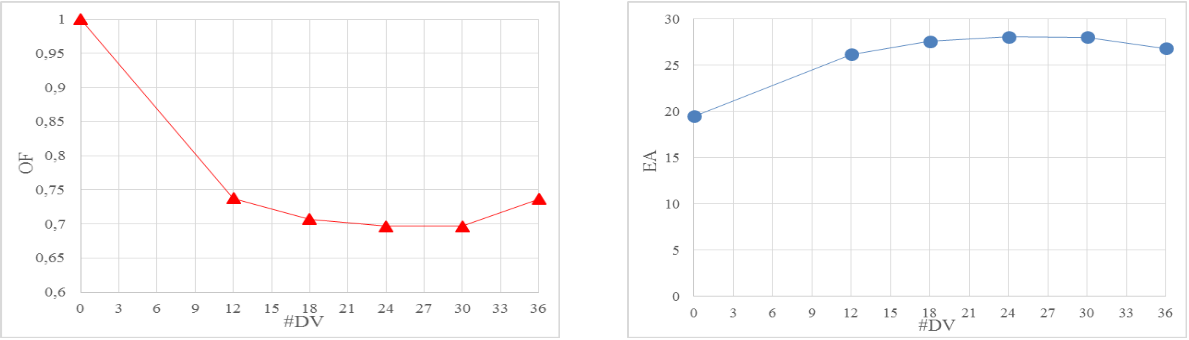

Figure 6. Evolution of OF and AE with #DV for DPW-W1 optimization

For this test case, only the upper face CPs have been considered. A single-point optimization has been executed for each parameterization. Results show that the optimum is reached when using 30 DV (10 DV at the upper face of each section) achieving an improvement by ~30% on OF, while the constrains on C_L and C_M have been fulfilled.

Figure 7 shows the shapes and pressure coefficient distributions of the original and optimized geometries

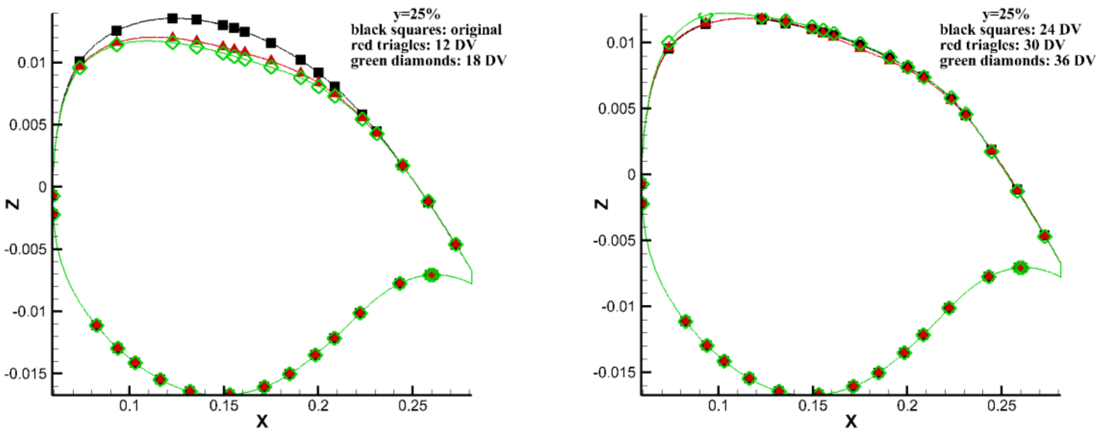

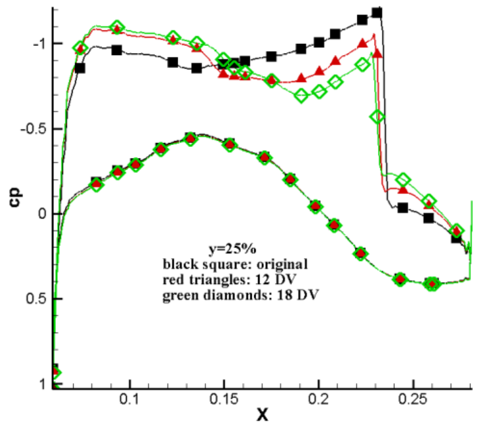
y=25%
black square: original
red triangles: 12 DV
green diamonds: 18 DV
cp
-1
-0.5
0
0.5
1
0.1
0.15
0.2
0.25
X

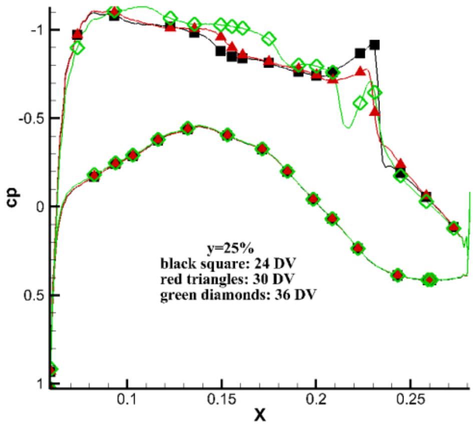
y=25%
black square: 24 DV
red triangles: 30 DV
green diamonds: 36 DV
cp
-1
-0.5
0
0.5
1
0.1
0.15
0.2
0.25
X

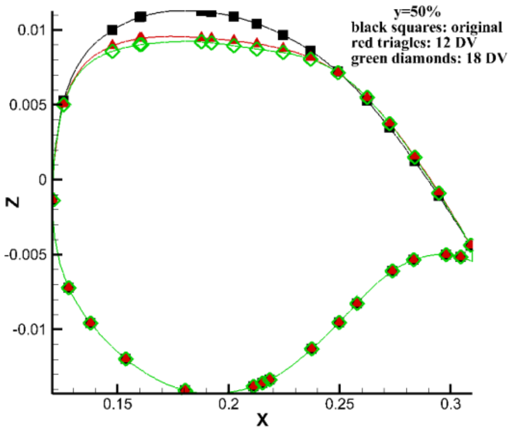
y=50%
black squares: original
red triagles: 12 DV
green diamonds: 18 DV
Z
0.01
0.005
0
-0.005
-0.01
0.15
0.2
0.25
0.3
X

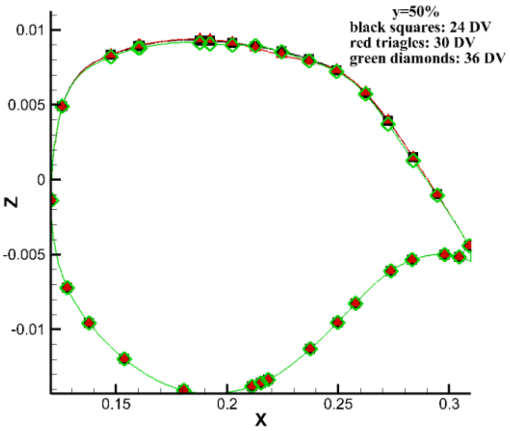
y=50%
black squares: 24 DV
red triagles: 30 DV
green diamonds: 36 DV
Z
0.01
0.005
0
-0.005
-0.01
0.15
0.2
0.25
0.3
X

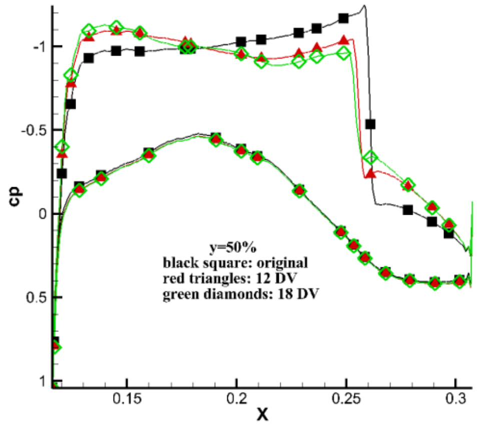
y=50%
black square: original
red triangles: 12 DV
green diamonds: 18 DV
cp
-1
-0.5
0
0.5
1
0.15
0.2
0.25
0.3
X

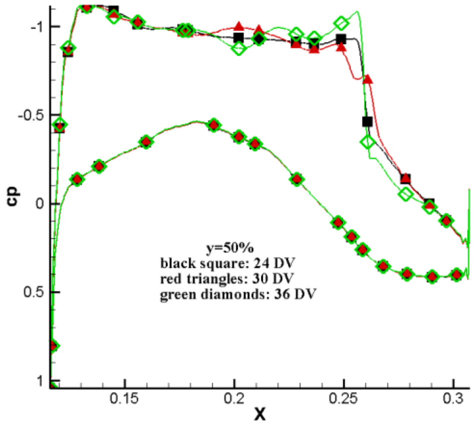
y=50%
black square: 24 DV
red triangles: 30 DV
green diamonds: 36 DV
cp
-1
-0.5
0
0.5
1
0.15
0.2
0.25
0.3
X

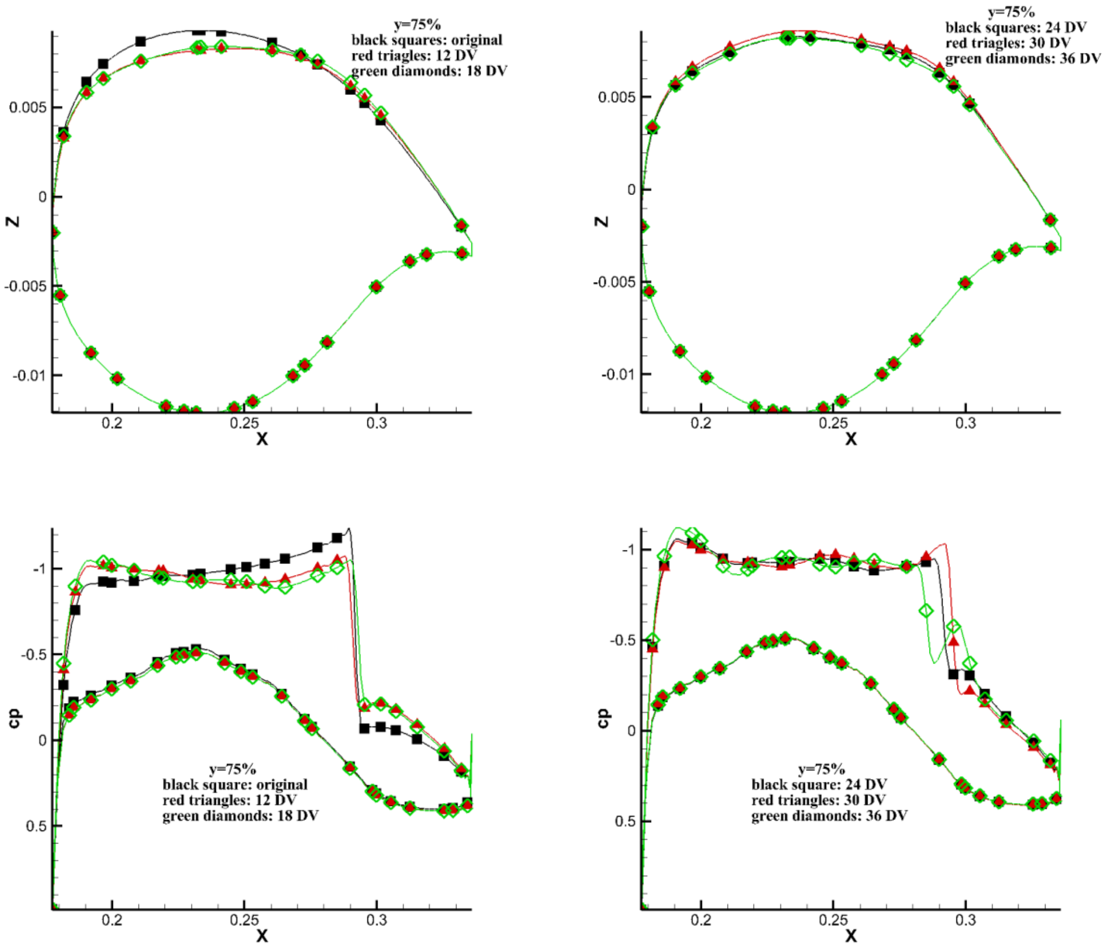

Figure 7. DPW-W1 wing optimization results

4.5. Execution time

The following formula approximates the computational time required by the proposed approach as a combination of the simulation time, the training time and the optimization time.

$$\begin{gathered} time = 5(simulation\ time) + (max\ CFD\ simulations - 5) \times \\ (training\ time + optimization\ time + simulation\ time) \end{gathered} \tag{14}$$

Table 5. Execution time considerations on a Linux x86_64 computational cluster

	RAE2822 **(RANS, 27k points)**	**DPW-W1** **(Euler, 427k points)**
Training time	~ 10 s.	~ 10 s.
Optimization time	~ 60 s.	~ 60 s.
Simulation time	30 s.+150 s. (8 processors)	300 s. (8 processors)
TOTAL APPROX	6.8 hours	30.7 hours

5. Conclusions

The aim of this work was to provide a comprehensive study about how the selected parameterization and number of design variables affect the convergence and results of surrogate-based global optimization methods (SBGO). The following conclusions have been extracted from the results:

- As expected, the selection of the design parameters and is a crucial step, and strongly determines the range of solutions and performance of the optimization algorithm.
- The optimal number of design parameters for defining a 2D airfoil geometry (i.e RAE2822) is between 10-12 DVs In addition, between 8DVs and 14DVs there is not a huge change in optimization performance.

For the 3D wing (DPW test case), the optimum is reached when using 30DVs (10 parameters in the upper-side of each section).Again, between 18DVs and 30DVs there is not a huge change in optimization performance.
Future work will extend this analysis by analyzing how sensitive this approach is to the location of the control points. Furthermore, the DPW in viscous flow conditions will be covered in order to validate these results. In addition, the proposed methodology will be also applied to the optimization of a 2D circle, in order to test the capability of this method to reach innovative shapes, and how different parameterizations will behave, when considering different objective functions.

Acknowledgements

The research describer in this paper made by INTA and UAH researchers has been supported under INTA activity *"Termofluidodinámica"* (IGB99001).

References

[1] J. Samareh, "A survey of shape parametrization techniques," in *CAES/AIAA ATIO Conference*, Anchorage, USA, 2008.

[2] P. Catonguay and S. Nadarajah, "Effect of shape parametrization on aerodynamic shape optimization," in *45th AIAA Aerospace Sciences Meeting and Exhibit*, Reno, 2007.

[3] H. Sobieczkt, "Parametric airfoils and wings," *Notes on Numerical Fluid Mechanics,* vol. 16, pp. 71-78, 1998.

[4] B. Kulfan, "Universal parametric geometry representation method-CST," in *45th AIAA Aerospace Science Meeting and Enxhibition,* Reno, 2007.

[5] J. Lepine and J. Trepanier, "Wing aerodynamic design using an optimized NURBS geometrical representation," in *38th AIAA Aerospace Science Meeting and Exhibit*, Reno, 2000.

[6] M. Martin, E. Andrés, M. Widhalm, P. Bitrian and C. Lozano, "Non-Uniform Rational B-Splines based aerodynamic shape optimization with DLR TAU code," *Proceedings of the Institution of Mechanical Engineers, part G, Journal of Aerospace Engineering,* vol. 226, no. 10, pp. 10-13, 2012.

[7] D. Chauhan, C. Praveen and R. Duvigneau, "Wing Shape Optimization Using FFD and Twist Parametrization," *Aerospace Sciences and Technologies,* pp. 225-230, 2010.

[8] M. Martin, E. Andrés, E. Valero and C. Lozano, "Volumetric B-splines shape parametrization for aerodynamic shape," *Aerospace Science and technology,* vol. 37, pp. 26-36, 2014.

[9] A. Mousavi, P. Castonguay and S. Nadarajah, "Survey of shape parameterization techniques and its effect on three-dimensional aerodynamic shape optimization," in *AIAA Computational Fluid Dynamics*, Miami, 2007.

[10] L. Piegl and W. Tiller, The NURBS book, New York: Springer-Verlag Berlin Heidelberg, 1997.

[11] J. Smith, "On replacement strategies in steady state evolutionary algorithms," *Evolutionary Computation,* vol. 15, no. 1, pp. 29-59, 2007.

[12] E. Ortiz-García, S. Salcedo Sanz, Á. Pérez-Bellido and J. Portilla-Figueras, "Improving the training time of support vector regression algorithms through novel hyper-parameters searchspace reductions," *Neurocomputing,* vol. 72, p. 3683–3691, 2009.

[13] E. Andrés, S. Salcedo-Sanz, F. Mongue and A. Pérez-Bellido, "Efficent aerdoynamic design through evolutionary programming and support vector regression algorithms," *Expert Systems with Applications,* vol. 39, pp. 10700-10708, 2012.

[14] DLR Institut of Aerodynamics and Flow Technology, "Technical Documentation of the DLR TAU-Code," Braunschweig, 2014.

[15] E. Andrés, L. Carro and S. Salcedo, "Fast aerodynamic coefficient prediction using SVMs for global shape optimization," in *ECCOMAS*, Barcelona, 2014.